Physiology & Behavior 147 (2015) 348–358

Contents lists available at ScienceDirect

Physiology & Behavior

journal homepage: www.elsevier.com/locate/phb

Interpersonal strategies for disturbance attenuation during a rhythmic joint motor action

A. Melendez-Calderon [a,c,*], V. Komisar [b,c], E. Burdet [c]

[a] Department of Physical Medicine and Rehabilitation, Northwestern University, USA
[b] Institute of Biomaterials and Biomedical Engineering, University of Toronto, Canada
[c] Department of Bioengineering, Imperial College of Science, Technology and Medicine, UK

HIGHLIGHTS

- We studied how physically-connected pairs of subjects attenuate mechanical noise.
- We proposed a novel way to analyze strategies based on interaction torques and EMG.
- In unperturbed trials, no global strategy but rather pair-specific strategies
- In perturbed trials, increased int. torques rather than independent co-contraction
- Pair performance was not consistently better than individual performances.

ARTICLE INFO

Article history:
Received 26 June 2014
Received in revised form 23 April 2015
Accepted 24 April 2015
Available online 8 May 2015

Keywords:
Interpersonal coordination
Human–human interaction
Joint motor action

ABSTRACT

Helping someone carry a table is fairly easy; however, our understanding of such joint motor actions is still poorly understood. We studied how pairs of human subjects (referred to as *dyads*) collaborate physically to attenuate external mechanical perturbations during a target tracking task. Subjects tracked a target moving in a slow and predictable way using wrist flexion/extension movements, with and without destabilizing torque perturbations. Dyad strategies were classified using interaction torques and muscular activity. During unperturbed interactions (baseline), the dyads tended to stabilize on a particular strategy. The baseline strategy was not the same in all dyads, suggesting that the solution to the task was not global but specific to each particular dyad. After several trials of unperturbed interactions, we introduced mechanical vibrations and analyzed the adaptation process. Dyads showed a tendency to counteract the external disturbances by first increasing co-contraction within each subject (independent co-contraction), and then raising the amount of opposing interaction torques (dyadic co-contraction) with increased perturbation amplitude. The introduction of perturbations impelled dyads to abandon their unperturbed baseline strategy and adopt a more common strategy across dyads, suggesting attractor solutions. Our results establish a framework for future human–human interaction studies, and have implications in human motor control as well as human–robot and robot–robot interactions.

1. Introduction

Humans are innately social beings and rely on inter-human interactions to accomplish tasks or learn new skills. These interactions are facilitated through a combination of communication means, including audition and language (e.g., two football referees making a joint-decision about a doubtful play), vision (e.g., a coach demonstrating a move which observing novice players are expected to emulate) or haptics (e.g., a father holding his child to help him/her keeping balance on the bicycle). In the context of motor skill acquisition, physical contact is recognized as a valuable means of helping others to gain motor skills and accomplish tasks. Physiotherapists training with patients are a common example of physical interpersonal interaction.

Joint motor interactions involve frequent or continuous exchange of haptic information and coordination between individuals. While language and gestural communication have been the subject of much research, very few studies have investigated physical interpersonal coordination strategies. Although the knowledge of joint action across physically-connected humans is growing [1–9], little is still known about how a pair of subjects (*dyad*) deals with noise and adapts their behavior to such disturbance when they are mechanically coupled [6]. Identifying these mechanisms is critical to develop efficient collaborative behavior of social robots in contact with humans (e.g. cooperative

* Corresponding author at: Abbott Hall Suite 1022, 710 N Lake Shore Drive, Chicago, IL, 60611. USA.
E-mail address: alejandro.melendez@northwestern.edu (A. Melendez-Calderon).

http://dx.doi.org/10.1016/j.physbeh.2015.04.046
0031-9384/

strategies in robot-assisted therapy) or between robotic agents, and to better understand the mechanisms of human motor control.

In an individual motor task, subjects deal with noise and instability by controlling the endpoint impedance through coordinated muscle activations [10–12]. When two subjects carry out a joint motor task while being mechanically connected, either directly or through an object, this dyad's mechanical impedance can be controlled using various strategies [6]. For example, one partner can co-contract while the other relaxes, both partners can co-contract to varying degrees (*independent co-contraction*), or partners can pull or push against each together (*dyadic co-contraction*). Therefore, a dyad has kinematic and muscle redundancy, both of which have been little-examined.

In this study, we investigated how the two subjects of a dyad performing a task while being mechanically-coupled deal with mechanical perturbations and adapt their behavior to counteract such disturbance. To investigate the different strategies that dyads use to attenuate these perturbations, we carried out experiments in which two subjects had to track a slow and predictable moving target using wrist flexion/extension movements while being mechanically-coupled— similar to the common command system of the pilot and co-pilot in old planes [13]. After several trials of unperturbed interaction, a sinusoidal torque perturbation was introduced and the strategies that subjects used to deal with the disturbance were analyzed. In addition to these *dyad sessions*, subjects performed the same tracking task in *individual sessions*, which allowed us to analyze the extent of independent co-contraction used during dyad sessions.

The results suggest that roles among partners are not inherent to the individual capabilities, but rather emerge between partners and are thus dyad-specific. We observed a general trend for dyads to stabilize on a particular strategy during natural (i.e. unperturbed) interaction. This baseline strategy was different for all dyads, suggesting that the solution for the task was not global but specific to each particular dyad. Furthermore, when mechanical noise was introduced, dyads showed a tendency to counteract these external perturbations by first increasing independent co-contraction, and then increasing the amount of opposing interaction torques (dyadic co-contraction), thereby impelling dyads to abandon their unperturbed baseline strategy and adapt a more common strategy across dyads.

2. Materials and methods

2.1. Subjects

Ten right-handed subjects (aged 21–31 years; 8 females) participated in this study. All subjects were naïve to the experimental conditions and had no known neuromuscular disorders or recent injury to the right wrist. Experiments were performed at the Department of Bioengineering of Imperial College London. The study was approved by the ethics committee of Imperial and all subjects gave their informed consent prior to participation.

Subjects were paired based on similar height and weight. *Dyads* were composed of four female pairings and one male pairing. All subjects participated in both *individual sessions* (IS) and *dyad sessions* (DS) as described in Sections 2.2 and 2.3 (experimental setup and protocol). Two dyads completed the IS the day before their DS, while two other dyads completed them the day after. In the remaining dyad, one partner completed her IS the day before the DS and the other, the day after.

2.2. Setup

Experiments were conducted on the Hi5 interface [14], which consists of two mechanically coupled wrist interfaces fixed to a table on which subject(s) place their arm, hold a handle, and interact with wrist flexion/extension movements (Fig. 1). These interfaces are equipped with DC motors (without reduction gears) that allow the experimenter to program external torques to the wrist joint. The coupling of the interfaces was done through a rigid, carbon fiber tube that connected the rotating shafts of the interface. Torque sensors (TRT-100, Transducer Technologies, USA) were mounted between the rotating shaft and the handle of each device. The two signals acquired from these sensors are referred as *interaction torques*.

The experiments required individual subjects or pairs of subjects (dyads) to track a target moving slowly and periodically on a computer monitor (represented by a solid green polygon) with a cursor that followed their wrist angular position (represented by a blue line) as shown in Fig. 1. During individual sessions subjects had to track the moving target using their dominant hand alone. During dyad sessions, the two subjects of a dyad had their handles rigidly-connected via a carbon fiber tube and moved the same cursor using their dominant hand. Subjects received visual feedback on independent displays.

For both individual and dyad sessions, participants were informed that they would experience forces in the apparatus coming through another apparatus connected through the carbon fiber tube. They were not told whether they were acting alone or in a pair. Subjects of a dyad did not meet each other prior or during the experimental sessions. To avoid non-haptic interactions, a heavy curtain suspended between the two wrist interfaces restricted vision and participants wore ear protections which attenuated auditory noise. To prevent individuals from knowing whether they were alone or interacting with another person at the beginning of the experiment, participants were asked to meet the experimenters in different rooms; this allowed them to enter the testing environment without seeing each other. Instructions to participants (e.g. move to target and relax) were delivered through visual messages that appeared on each of the subjects' personal screen instead of relying on verbal instructions, which could have made subjects aware about the presence of another person.

Wrist angular position and interaction torques were recorded at 100 Hz, while surface electromyography (sEMG) from both *flexor carpi radialis* (FCR) and *extensor carpi radialis longus* (ECR) muscles on the right forearm was recorded at 1000 Hz (see Section 2.4). In our descriptions and figures, the partners standing in the left and right positions are described as *green partner* (G) and *yellow partner* (Y), respectively.

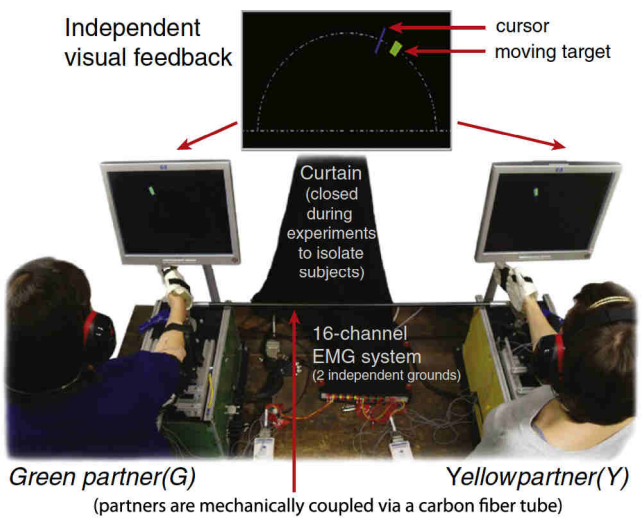

Fig. 1. Overview of the experimental rig —*Hi5*. The figure shows a dyad performing a collaborative tracking task. Partners are mechanically coupled by holding handles connected with a carbon fiber tube. Surface EMG, interaction torques and kinematic data are recorded from both participants. Subjects are about 1 m away. They are separated by a curtain and wear hearing protection to avoid non-haptic interactions.

2.3. Protocol

Each experimental session consisted of an EMG calibration procedure (see Section 2.4) followed by thirty 20 s tracking trials. Within each trial, a target moved periodically at 0.2 Hz ($T = 5$ s) from $-20°$ to 20° with a smooth angle trajectory:

$$\theta(t) = \begin{cases} \frac{7680t^5}{T^5} - \frac{9600t^4}{T^4} + \frac{3200t^3}{T^3} - 20 & 0 \le t < \frac{T}{2} \\ -\frac{7680\,(t-\frac{T}{2})^5}{T^5} + \frac{9600\,(t-\frac{T}{2})^4}{T^4} - \frac{3200\,(t-\frac{T}{2})^3}{T^3} + 20 & \frac{T}{2} \le t < T \end{cases} \quad (1)$$

$$\theta(t) = \theta(t+T).$$

Note that each wrist motion from $-20°$ to 20° or from 20° to $-20°$ corresponds to a minimum jerk trajectory [15] and can be visualized in Fig. 3 (first column).

During trials 11 to 30, an external 3 Hz sinusoidal torque perturbation of different amplitudes was applied to the subjects' wrist joint by the robotic device. For the first 10 trials, no torque perturbation was applied (Level 1); for the subsequent block of 10 trials (Level 2), 0.5 N·m (DS) and 0.25 N·m (IS) were applied; and finally, for the last 10 trials in the experiment (Level 3), 1 N·m (DS) and 0.5 N·m (IS) were applied. To minimize possible effects of fatigue, subjects were given a 20 s rest period between trials.

To begin a trial, participants were instructed on the screen to move the cursor to the target's initial position (located at $-20°$) and relax. After ensuring that participants were comfortably relaxed in the target for at least 1 s, recordings of 2 s in the resting state were taken. The screen then displayed a 3 s countdown, followed by target movement to begin the tracking trial. Trials began with the target moving in the counter-clockwise (CCW) direction towards 20° (first 2.5 s of the trial), then moving periodically between 20° and $-20°$ at 0.2 Hz (middle 12.5 s), and finishing clockwise (CW) movement from 20° to $-20°$ (last 2.5 s of the trial). The target width was 4° for all levels.

Subjects were instructed to "try to keep the cursor inside the moving target" throughout the whole duration of the trial. The percentage of time that a dyad spent inside the target was displayed on the computer screens of the two partners after each trial. To motivate subjects' attention to the task, subjects were told that they would obtain a monetary reward based on their performance at the end of the experiment. However, all subjects received a lunch voucher equivalent to 5 GBP per experimental session, regardless of their performance.

2.4. Electromyography

Surface electromyography (EMG) was measured from *flexor carpi radialis* (FCR) and *extensor carpi radialis longus* (ECR), two major contributors to wrist flexion and extension in a midway position [6]. After the electrode position was determined for each muscle using functional movements, the area was cleansed with alcohol and abrasive gel (Nuprep, DO Weaver, Weaver and Company, USA). Disposable pregelled adhesive electrodes (Kendall/Tyco H135SG) were fixed to the subject's skin (inter-electrode distance: ~1 cm) and a ground electrode was fixed on the subject's ulnar head. The EMG signals were preamplified using active clip connectors (g.GAMMAclip + g.GAMMABox, g.Tec, Austria) and amplified using a medically-certified amplifier (g.BSamp, g.Tec, Austria). Signals were recorded at 1000 Hz using a National Instruments data acquisition card (NI 6221, National Instruments, USA). For subsequent analysis, EMG data were processed offline. A zero-lag fourth-order 20–500 Hz band-pass Butterworth filter was first used to filter out cable movements' artifacts and high frequency noise components. The signal was then rectified and low-pass filtered using a zero-lag fourth order Butterworth filter with 5 Hz cut-off frequency.

2.4.1. Calibration procedure

Each subject started the experiment with a four-partEMG calibration procedure consisting of: *i*) relaxation, *ii*) flexion, *iii*) extension and *iv*) co-contraction sessions. This procedure allowed for normalization of the EMG signals, thereby facilitating comparisons between participants' muscular activity and contributions to the collaborative task. Each part of the calibration lasted for 4 s; the last 2 s of each recording was used to calculate the parameters for the normalization of FCR and ECR. A rest time of 20 s was given between parts. The whole calibration procedure was conducted five times (five *calibration sessions*), with 60 s of rest given between consecutive sessions to avoid fatigue. The four parts consisted of:

i) *Relaxation*— subjects were asked to relax their forearms as much as possible and not move. The device was blocked at 0° and subjects had visual feedback of their applied torque so as to motivate them to keep relaxed.

ii-iii) *Flexion–extension*— subjects were instructed to either flex or extend their wrist and keep a constant level of torque while the device was blocked at 0°. The torque level required from the subjects varied from 1 to 5 N·m (i.e. 1 N·m in session 1, 2 N·m in session 2, and so on). A cursor was programmed to respond to individual torque measurements amplified fourfold (i.e., 1 N·m of applied torque moved the cursor by 4°), which provided subjects with visual feedback of the applied torque level. Subjects were asked to apply the force necessary to keep the cursor inside a target.

iv) *Co-contraction*— subjects were asked to co-activate maximally and to try to keep the cursor within the target positioned at 0° (target width: 4°) during 4 s. To help subjects achieve their maximum voluntary co-contraction (MVCC) level, the device perturbed the wrist. The perturbation consisted of a 0°-centered, 3 Hz sinusoidal trajectory of 10° amplitude using a PD controller ($K_p = 28.6$ N·m/rad and $K_d = 0.01$ N·m·s/rad).

2.5. Interpersonal coordination strategies based on interaction torques

For the analysis of interaction torques we partition the data as follows. Given that a dyad tracked a target moving back and forth from $-20°$ to 20°, we defined the tracking attempt from $-20°$ to 20° or from 20° to $-20°$ as a *motion*. Motions from $-20°$ to 20° were described as *counter-clockwise motions*, while motions from 20° to $-20°$ were described as *clockwise motions*. A *sweep* was defined as two successive motions from $-20°$ to 20° and back to $-20°$.

We developed an ad hoc algorithm that classified the interaction torques' temporal profiles into categorical strategies (Appendix A—classification of specific strategies based on interaction torques). The method consists of comparing normalized interaction torques against pattern templates that resemble recurrent patterns of interaction torques observed during the experiment. Similar to a nearest neighbor classifier, our algorithm computes the Euclidean distance between a test sample and the set of templates. We define the likelihood that a given dyad has adopted a particular strategy to be inversely-proportional to this distance. In addition, within these strategies dyads can modulate the overall impedance by sharing different amounts of muscle co-contraction. The contribution in terms of co-contraction levels of each partner adds specificity to a description of a dyad's strategy.

2.6. Interpersonal coordination strategies based on muscle co-contraction

During individual sessions, the only way to attenuate the torque perturbations is by co-contracting antagonistic muscles. However, during *dyad sessions*, torque perturbations can be attenuated either by the *independent co-contraction* of the flexor and extensor muscles in each

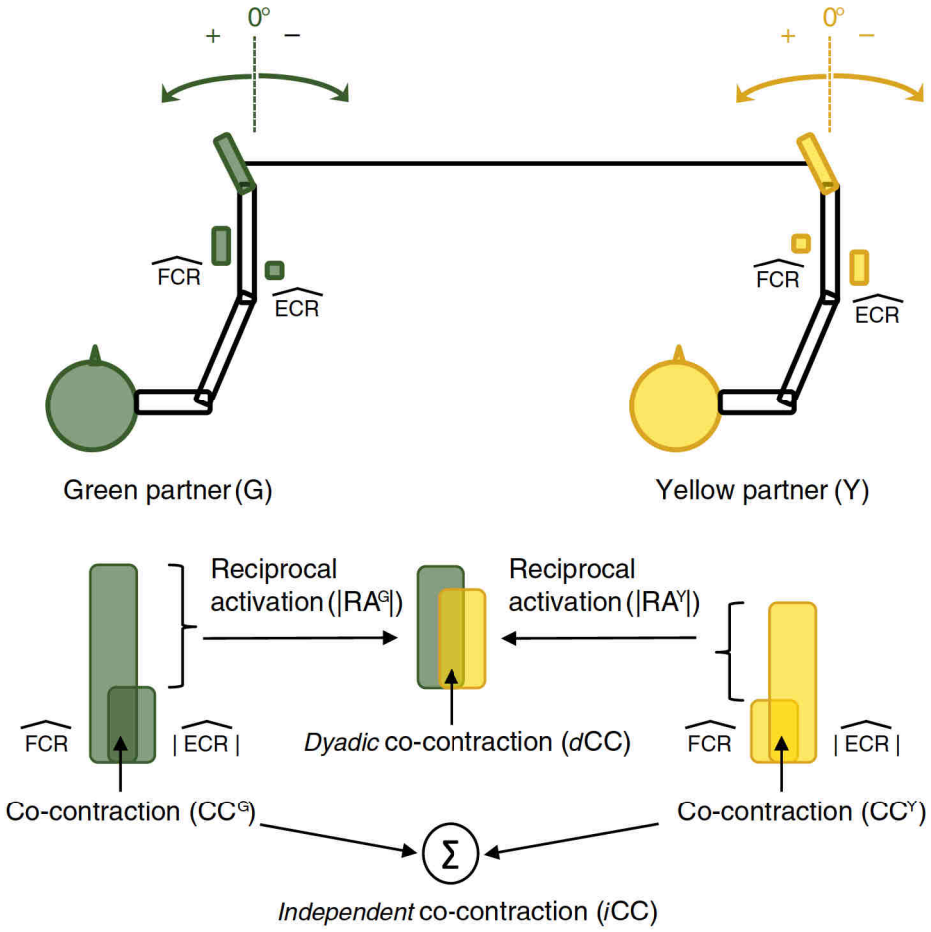

Fig. 2. During *dyad sessions*, partners can attenuate mechanical noise by two different types of co-contractions: *i*) independent or *ii*) dyadic. Independent co-contraction refers to each partner co-contracting antagonistic muscles. Dyadic co-contraction arises when partners generate opposing reciprocal activations.

partner, or by opposing reciprocal activation in the two partners (*dyadic co-contraction*), i.e. one partner contracts flexors and the other extensors, or vice-versa, as shown in Fig. 2. To analyze which of these strategies was used by the dyads, EMG signals were first normalized with respect to torque. Torque and rectified EMG signals recorded during the *relaxation*, *flexion* and *extension* phases of the EMG calibration were used to compute $\widehat{FCR}$ and $\widehat{ECR}$, which represent the normalized EMG activation with respect to the torque that it generates (a linear relationship was assumed). Note that $\widehat{FCR}$ is always positive and $\widehat{ECR}$ is always negative according to the torque sign convention. A partner's *co-contraction* (CC) was defined as the overlap of muscle activation, as

$$CC = \min\left(\widehat{FCR}, \left|\widehat{ECR}\right|\right). \tag{2}$$

Reciprocal activation (RA) was defined as:

$$RA = \widehat{FCR} + \widehat{ECR}. \tag{3}$$

The total amount of co-contraction during individual sessions is given by Eq. (2). During dyad sessions, the total amount of co-contraction (*t*CC) is the sum of each partner's individual co-contraction level (*independent co-contraction*— *i*CC) plus the co-contraction that arises as a result of opposing reciprocal activations between partners (*dyadic co-contraction*— *d*CC) (Fig. 2). This can be expressed as:

$$tCC = iCC + dCC \tag{4}$$

$$iCC = CC^{G} + CC^{Y} \tag{5}$$

$$dCC = \begin{cases} \min\left(\left|RA^{G}\right|, \left|RA^{Y}\right|\right), & \text{if } \operatorname{sgn}\left(RA^{G}\right) \neq \operatorname{sgn}\left(RA^{Y}\right) \\ 0, & \text{else} \end{cases}. \tag{6}$$

In our subsequent analysis, *i*CC and *d*CC levels of each dyad were normalized by the sum of maximum co-contraction levels, *m*CC, achieved by each partner during individual sessions as:

$$\widehat{dCC} = \frac{dCC}{mCC} \tag{7}$$

$$\widehat{iCC} = \frac{iCC}{mCC} \tag{8}$$

$$mCC = \max_{k}\left(\overline{CC}_{k}^{G,IS}\right) + \max_{k}\left(\overline{CC}_{k}^{Y,IS}\right) \tag{9}$$

where $\overline{CC}_k$ corresponds to the mean co-contraction level of a trial *k*.

3. Results

3.1. Interpersonal coordination strategies based on interaction torques

3.1.1. Patterns of interaction torques

We observed recurrent regularities on the interaction torques generated by dyads within a sweep. To capture these patterns, we classified the interactions according to five categorical patterns (Fig. 3, as in

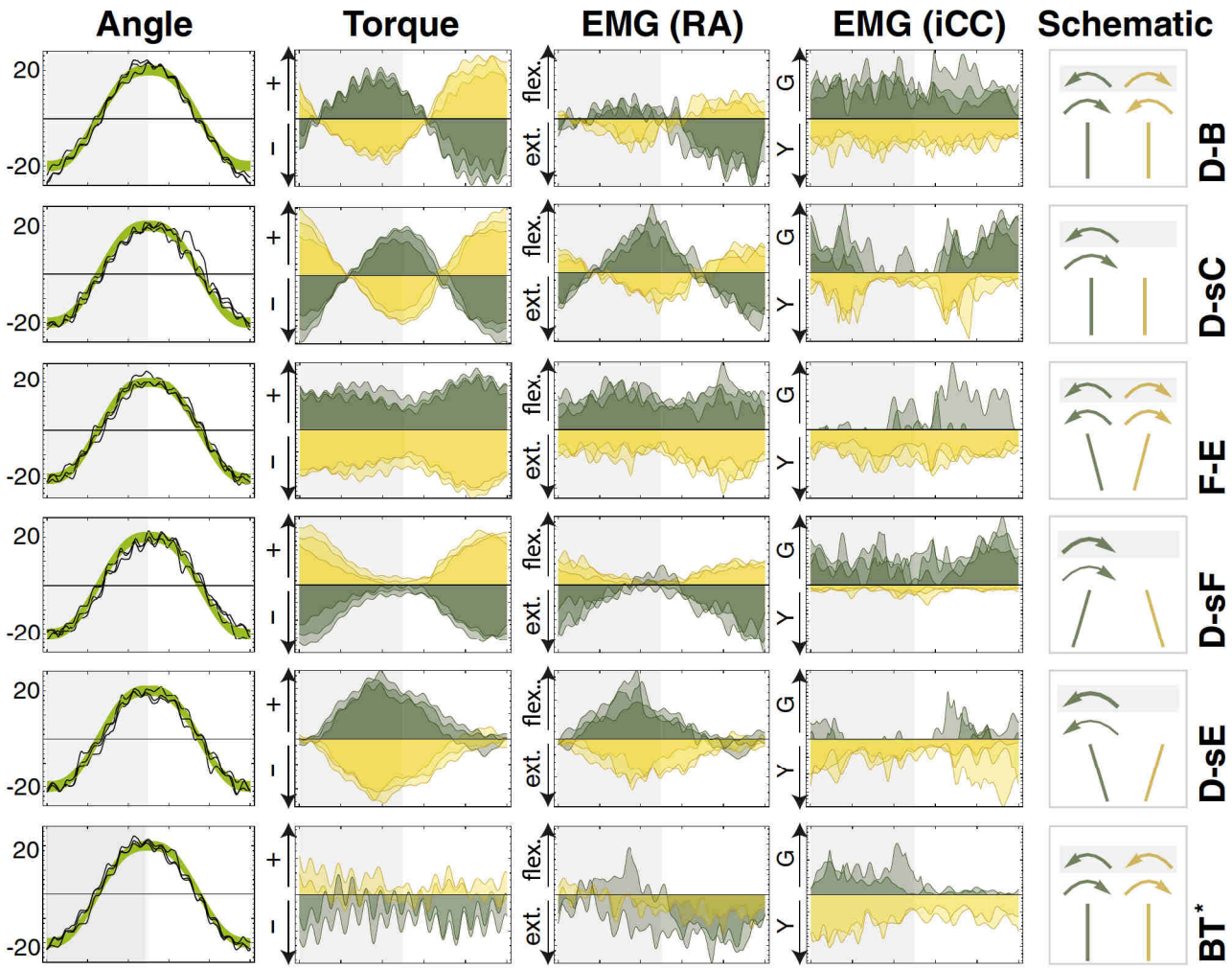

Fig. 3. Characteristic patterns observed in dyads during the experiment. These specific examples were obtained with torque perturbations set at 0.5 N·m. The patterns showed are relative to the green participant (e.g. the D–B pattern in this figure means that the green partner is driving and the yellow partner braking). The gray and white background rectangles denote CCW and CW motions respectively. *Note that the BT example does not exhibit a particular pattern and therefore, it is considered a special case (see text for details).

[6]): *i*) Drive and brake (D–B); *ii*) drive and stay centered (D–sC); *iii*) flex and extend (F–E); *iv*) drive and stay flexed (D–sF); and *v*) drive and stay extended (D–sE). A special category, both try (BT), was included when the measured data did not match (reliably) any of the main five categories. These categories were defined based on thorough observations during preliminary trials. We chose descriptive names that correspond to roles/actions that would generate the observed interaction torque patterns, but they do not necessarily correspond to the subjects' intentions — which is beyond the scope of this study. Each pattern is described in further detail below.

3.1.1.1. Drive and brake (D–B). This pattern is characterized by interaction torques that are positive for one partner – D role – and negative for the other partner – B role – during counter-clockwise motions, but the torque signs are inverted during clockwise motions. This pattern exhibits zero crossings in the interaction torque profiles at approximately the beginning, middle and end of each sweep (i.e. beginning and end of each motion, i.e. cursor at ~20° and ~−20°), when the target changes direction. The pattern looks like sine-waves with ~0°phase-shift for one partner and ~180°phase-shift for the other. This characteristic pattern would be observed if one of the partners moves the cursor, while the other actively retards and/or stabilizes the movement regardless of the motion direction. If the movement is sufficiently slow, as in the case of our task (2.5 s per motion), this action generates an interaction torque for one partner with a sign consistent to the direction of the movement, and the interaction torque for the other partner would be opposite in sign and roughly equal in magnitude. The synchronization between partners' torques produces the zero crossings described earlier when both partners – who are assuming active roles – also change the direction in which they apply torques.

3.1.1.2. Drive and stay centered (D–sC). This pattern is characterized by interaction torques that are 90°phase-shifted from a D–B pattern, i.e. the pattern looks like sine-waves with a zero crossing at approximately the middle of each motion (i.e. cursor at ~0°), with the magnitudes of the interaction torques being highest at the end of each motion (i.e. cursor at ~20° and ~−20°). This characteristic pattern would be observed if only one partner (e.g. green) maintains an active role in guiding cursor motion in both directions —D role, while the other (e.g. yellow) seems to be trying to keep a fixed position at 0°— sC role. In this scenario, the yellow partner could be not making a significant attempt to control cursor motion (e.g. s/he stays relaxed or focuses instead on increasing wrist stiffness through co-contraction to attenuate outside disturbances) or the braking torques applied by the yellow partner are not properly synchronized with both the green partner and moving target (as in D–B).

3.1.1.3. Flex and extend (F–E). This pattern is characterized by interaction torques that are consistently positive for one partner — F role and consistently negative for the other partner —E role. The magnitudes of the interaction torques are lowest at approximately the beginning, middle

and end of each sweep (i.e. beginning and end of each motion), when the target changes direction, and highest half-way through a motion. This characteristic pattern would be observed if one of the partners actively modulates flexion while the other extension in order to minimize interaction torques at the end of each motion. This would imply that one partner applies a torque to guide the cursor during one motion (e.g. from 20° to −20°) but applies an opposing torque to retard and/or stabilize the movement during a successive motion (e.g. from −20° to 20°), while the other partner does the opposite.

3.1.1.4. Drive and stay flexed (D–sF). This pattern is characterized by interaction torques that are consistently negative for one partner —D role and consistently positive for the other partner — sF role. The magnitudes of the interaction torques are lowest at ~20° and highest at ~−20°. This characteristic pattern would be observed when one partner (e.g. green under the D role) controls the cursor's motion by increasing or decreasing his/her extensor activity, while the other partner (e.g. yellow under the sF role) maintains a high state of flexion. In this scenario, interaction torque profiles would exhibit at a high magnitude when the target is farthest from the yellow partner's flexed position, and decrease to a minimum roughly halfway through the sweep, closest to the yellow partner's flexed position.

3.1.1.5. Drive and stay extended (D–sE). This pattern is characterized by interaction torques that are consistently positive for one partner —D role and consistently negative for the other partner — sE role. The magnitudes of the interaction torques are lowest at ~−20° and highest at ~20°. This characteristic pattern would be observed when one partner (e.g. green under the D role) modulates the movement by increasing or decreasing his/her flexor activity, while the other partner (e.g. yellow under the sE role) attempts to maintain a high state of extension.

3.1.1.6. Both-try (BT) — special case. When both partners try to move simultaneously in the direction of the moving target, the measured interaction torque may become too low and the interference caused by the unavoidable nonlinearities of the experimental rig – such as mechanical friction, damping and sensor hysteresis – may become significant. Therefore, while one could still try to classify the interaction torque profile into one of the previous patterns, the results could be easily misinterpreted. Therefore, the both try "pattern" is not a pattern per se, as the interaction torques do not show any sort of regularity. This class can be easily identified by looking at the percentage of the trial in which the dyad muscular reciprocal activations overlap. If the overlap is high and the measured interaction torques do not resemble any of the previous patterns, there is a high probability that the partners are trying to move simultaneously.

3.1.2. Strategies for disturbance attenuation

We say that a dyad is executing a particular strategy when the measured interaction torques during a sweep have been categorized according to the patterns described earlier and when the specific roles within the identified pattern have been assigned to each partner. For instance, when a D–B pattern is identified in the data and the green partner seems to be the driver, we could say that the dyad is executing a *green drives and yellow brakes* strategy. From this perspective, we define ten different *specific strategies* corresponding to the five patterns (D–B, D–sC, F–E, D–sF, D–sE): *i*) Green drives and yellow brakes (GD–YB), *ii*) yellow drives and green brakes (YD–GB), *iii*) green drives and yellow stays centered (GD–YsC), *iv*) yellow drives and green stays centered (YD–GsC), *v*) green flexes and yellow extends (GF–YE), *vi*) yellow flexes and green extends (YF–GE), *vii*) green drives and yellow stays flexed (GD–YsF), *viii*) yellow drives and green stays flexed (YD–GsF), *ix*) green drives and yellow stays extended (GD–YsE), and *x*) yellow drives and green stays extended (YD–GsE).

Given the dynamic nature of the interaction torques, we were interested in analyzing whether or not dyads would transition (or switch) between strategies during the experimental session. Therefore, we represented the space of possible strategies as a ring and allocated each strategy in the ring so that similar strategies were closer to each other (Fig. 4). From this arrangement, we also defined four *broad strategies*: *i*) pulling, *ii*) pushing, *iii*) green drives and *iv*) yellow drives.

3.1.2.1. Pulling strategy. This broad strategy corresponds to the upper sector of the strategy space. A "pure" *pulling* strategy would correspond to the specific strategy GF–YE, as if the partners were "pulling" the linking bar between them.

3.1.2.2. Pushing strategy. This strategy is completely orthogonal to the *pushing* strategy. This broad strategy corresponds to the lower sector of the strategy space. A "pure" *pushing* strategy would correspond to the specific strategy YF–GE, as if the partners were "pushing" (or compressing) the linking bar between them.

3.1.2.3. Green drives strategy. This broad strategy corresponds to the left sector of the strategy space. A "pure" *green drives* strategy would correspond to the specific strategy GD–YB.

3.1.2.4. Yellow drives strategy. This strategy is completely orthogonal to the *green drives* strategy. This broad strategy corresponds to the right sector of the strategy space. A "pure" *yellow drives* strategy would correspond to the specific strategy YD–GB.

Note that broad strategies are not intended to have sharp boundaries, the further away the measured interaction torque deviates from the strategies on each of these sectors, the less one can be certain that the partners are attempting a particular broad strategy.

Based on this taxonomy, interaction torques were classified as shown in Fig. 5 and described in detailed in Appendix A. Fig. 6 shows the evolution of strategies based on interaction torques over the course of the experiment. One can see that in the trials without mechanical perturbation (Level 1), all dyads tended to converge to a particular broad strategy, although transitions between neighboring specific

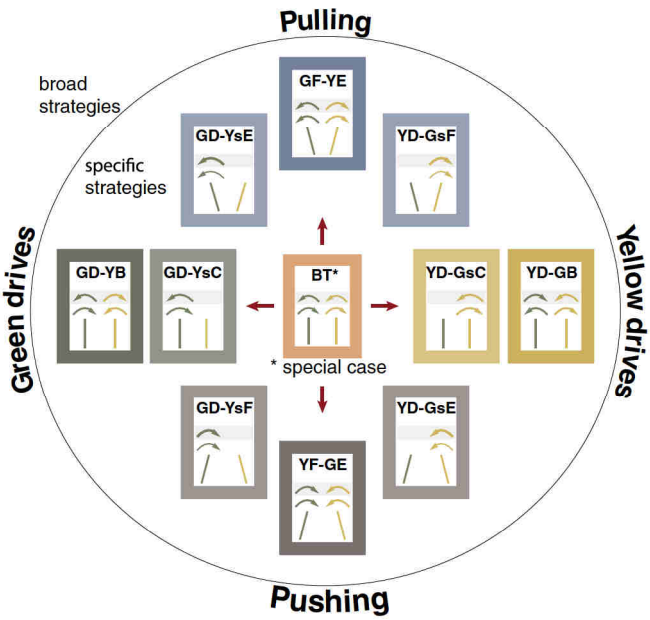

Fig. 4. Organization of strategies. Specific strategies are arranged based on their similarity. Transitions between neighboring strategies are more likely to happen than transitions between separate ones. Note that both try (BT) is a special case and it is not considered a specific strategy per se (see text for details). We define 4 broad strategies, *pulling*, *pushing*, *green drives* and *yellow drives* corresponding to the upper, lower, left and right areas of the ring, respectively.

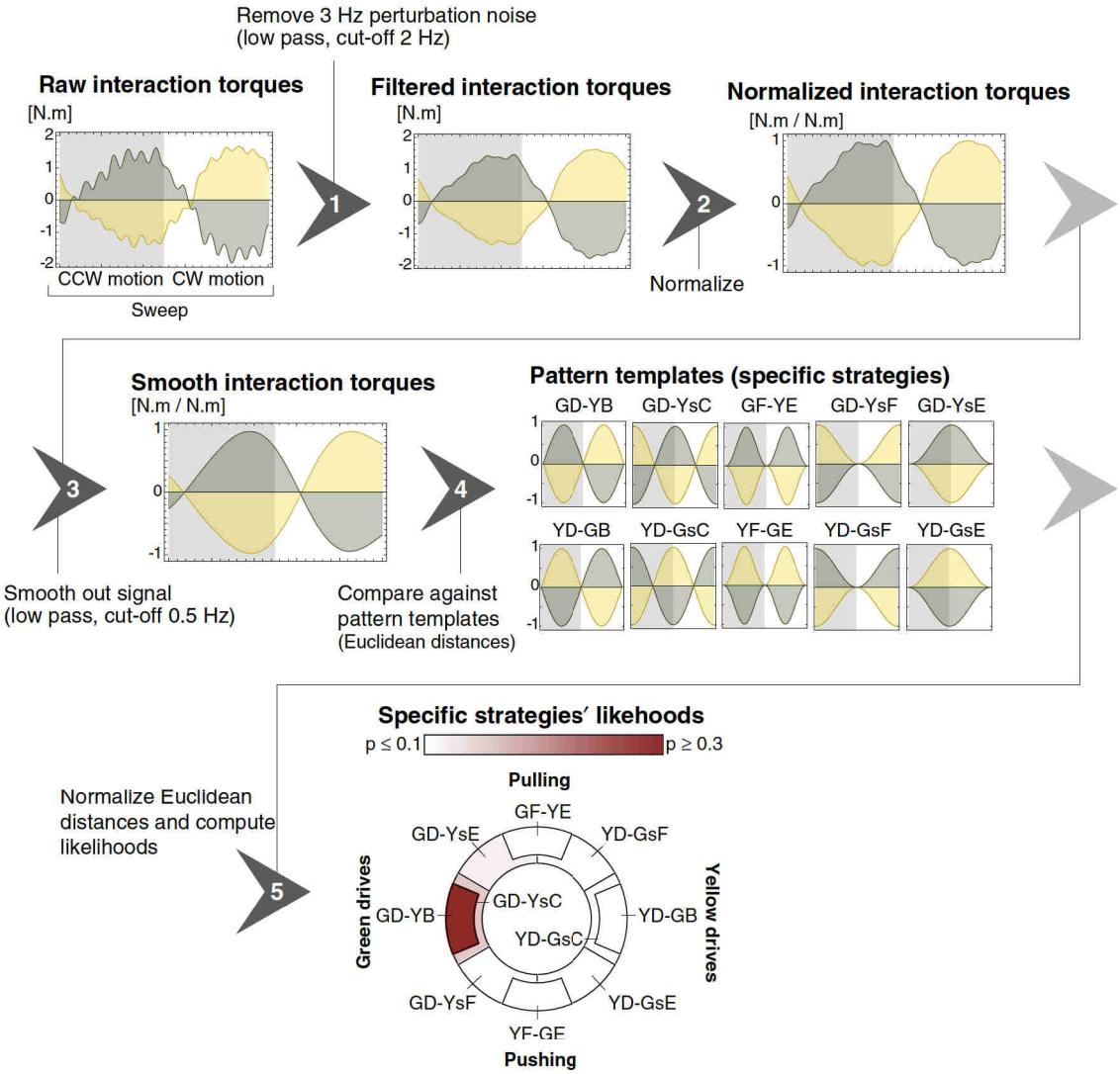

Fig. 5. Schematic of the specific strategy classification method based on interaction torques. See Appendix A for details.

strategies were also observed. Driver approaches (i.e. green drives or yellow drives strategies) dominated the behavior of dyads 2, 3 and 5. Dyad 4 converged to a pushing strategy, while dyad 1 converged to a pulling strategy. The introduction of external torque disturbances prompted dyads who adopted a driver approach to abandon their original strategy. As perturbation increased, all dyads tended to use strategies dominated by pushing or pulling approaches.

3.2. Interpersonal coordination strategies based on muscle co-contraction

Within the strategies based on interaction torques, dyads can modulate the overall impedance by sharing different amounts of co-contraction level. For example, as external perturbations of increasing magnitudes are applied, the overall impedance of the dyad can be varied by one partner applying a high level of co-contraction relative to the other, or by both partners applying comparable levels. Therefore, the contribution in terms of co-contraction levels of each partner adds further specificity to the specific and broad strategies described in the previous section.

Further analysis on EMG levels showed that the convergence to pushing or pulling strategy when mechanical perturbations were increased was not limited by the capacity of the subjects to attenuate disturbances by using independent co-contraction and maintain a specialized strategy. Fig. 7 shows the distribution of normalized co-contraction levels $\widehat{iCC}$ and $\widehat{dCC}$. When the tasks were carried out without torque perturbations, the partners used moderate independent co-contraction to ensure task stability and negligible dyadic co-contraction (except for dyad 1). When torque perturbations were introduced (Level 2), dyads tended to increase $\widehat{iCC}$ more than $\widehat{dCC}$ (two sided t-test, $p = 0.056$). Stronger torque perturbations (Level 3) were accompanied by a simultaneous increase of both $\widehat{iCC}$ and $\widehat{dCC}$, with a larger increase of $\widehat{dCC}$ (two sided t-test, $p = 0.065$). This strategy was not limited by the capacity of the subjects to attenuate disturbances by co-contracting independently. As illustrated in the figure, dyads kept $\widehat{iCC}$ levels below 1, meaning that they could have attenuated disturbances by independently co-contracting instead of increasing the interaction torques.

It is worth noting that the main purpose of these comparisons is not to simultaneously test and confirm a hypothesis. Hypotheses should not be formulated and confirmed within the same data set. Comparisons in an observational study, like ours, should only be

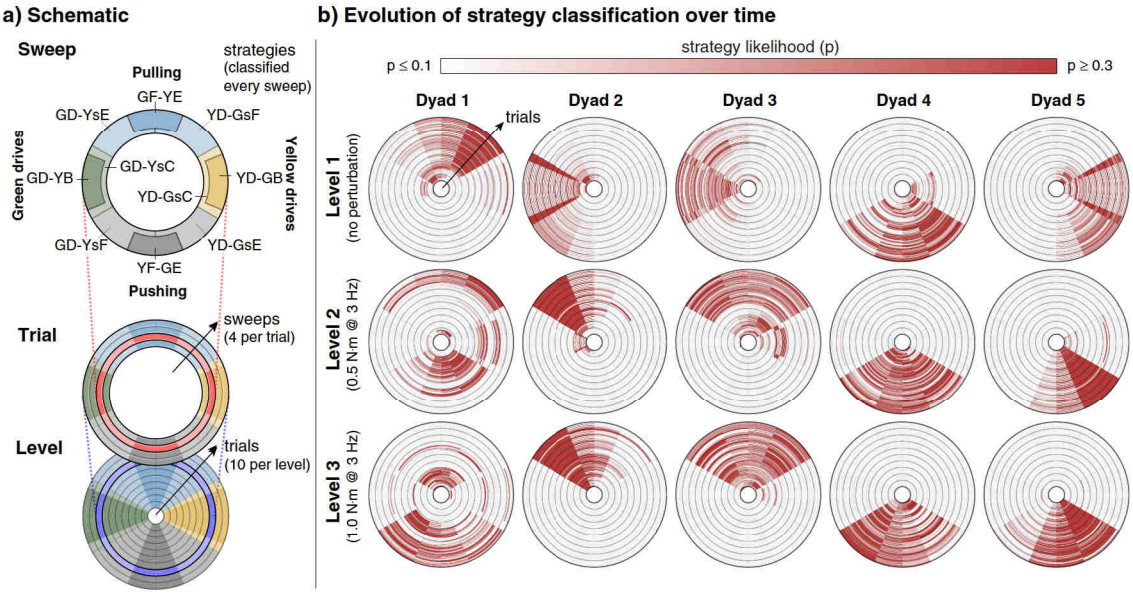

Fig. 6. a) Each circle in (b) represents a level; each *circle level* is divided in ten equally spaced rings representing trials (each trial lasted 20 s). Trial 1 starts at the middle of the *circle level*. Each *trial ring* is further sub-divided in four equally spaced rings representing the sweeps performed during a trial (a sweep is defined as two successive motions — from −20° to 20° and back to −20°; each sweep lasted 5 s). Each *sweep ring* has clusters representing the dyad strategies as in Fig. 4. b) Evolution of dyad strategies over time, during a periodic tracking task with different levels of external torque perturbation. The likelihood of a particular strategy for each sweep is calculated as shown in Fig. 5. The BT special case was not included in this analysis as likelihood values for the different specific strategies were always relatively high, indicating a low probability for a BT special case. Observe the tendency of the dyads to settle on a broad strategy and remain in the vicinity of neighboring specific strategies during unperturbed trials. Pushing and pulling strategies dominated the responses in trials with mechanical perturbations.

used to generate hypotheses to be tested in subsequent studies [16]. We have presented trends that are significant at the <10% level, which we found merit of reporting and motivate further investigation.

3.3. Individual vs dyadic performance

All dyads were able to track the $[-2°, 2°]$ moving target together at all difficulty levels. We did not find any relationship between the dyad strategy and task performance (as measured by tracking error). However, the tracking error variance during dyad sessions was consistently lower than the variance of the worse[1] partner (sign test, $p < 0.001$), but not consistently lower than the variance of the better partner (sign test, $p = 0.118$). In other words, the dyadic performance was, most of the time, better than the performance of the worse partner but worse that the performance of the better partner. Only in few cases, dyadic performance was better than the performance of the better partner.

4. Discussion

In this paper, we elucidated and characterized haptic interaction strategies that dyads use in undertaking a collaborative periodic tracking task while attenuating mechanical perturbations. We presented an analysis of ten individuals working in pairs and developed a quantitative classification system that automatically identified which strategy partners in a dyad were most likely to be undertaking during the task.

When two subjects physically interact with each other, distinct roles (e.g. dominant/non-dominant[17] and executor/conductor [4]) can be assigned to the interacting agents based on observed kinematic/dynamic patterns that emerge during the interaction. Through analyses of interaction forces, Reed and Peshkin [18] found that partners within a dyad develop roles such as "active/inert" (characterized by one partner initiating all velocity changes at appropriate times in the trial) and "specialized" (for which one partner would contribute more substantially to the acceleration phase of crank motion, while the other partner would adopt a more active role in the deceleration phase). A study conducted by Stefanov et al. [4] proposed alternative specializations to those identified by Reed and Peshkin. Stefanov et al. defined "execution" and "conductorship" as the main roles in a haptic interaction task. The former describes the partner who contributes most of the force for the task, while the latter refers to the partner who guides motion acceleration and indicates (through "haptic signals") when the dyad should change the direction of motion. Stefanov et al. similarly consider interaction forces along with kinematic trajectory data, using tristate logic and analytic expressions to assign executor and conductor roles based on the sign of the direction of object velocity and that of the interaction force applicable to each partner (with the third state accounting for cases where executor and conductor roles are not clear at different phases within a given trial). Groten et al. [5] followed this with a discussion of these dominance measures in haptic collaboration, where they investigated the consistency of dominance behavior between partners in trials with haptic/visual or visual-only feedback. They found that haptic feedback led to a more even dominance distribution between partners, in contrast with fairly consistent dominance/dominated behavior among partners when only visual feedback was present. They also found out that the switching between *dominant* and *non-dominant* behaviors was high during a dyad collaborative tracking task and concluded that dominant behavior seems to be more linked to the person rather than to the interaction parameters.

The broad classification method presented in our paper categorized dyad strategies with lower time resolution as in [18] and [4]. While the finer granularity of previous studies gives a good insight about low level interactions in time, it makes it difficult to analyze the data systematically when long, repetitive trials are being performed. In particular, using a finer granularity to analyze continuous control in relatively long trials would still require methods to interpreting this fine granularity at a higher level. In contrast, our broad classification allowed us to systematically analyze behavior at a comprehensive level, thereby facilitating the analysis and helping us to gain knowledge of why dyads might favor one particular strategy over another. Using our ad hoc

[1] We defined the "worse" partner as the one that had a higher tracking error variance during individual sessions as compared to his/her partner.

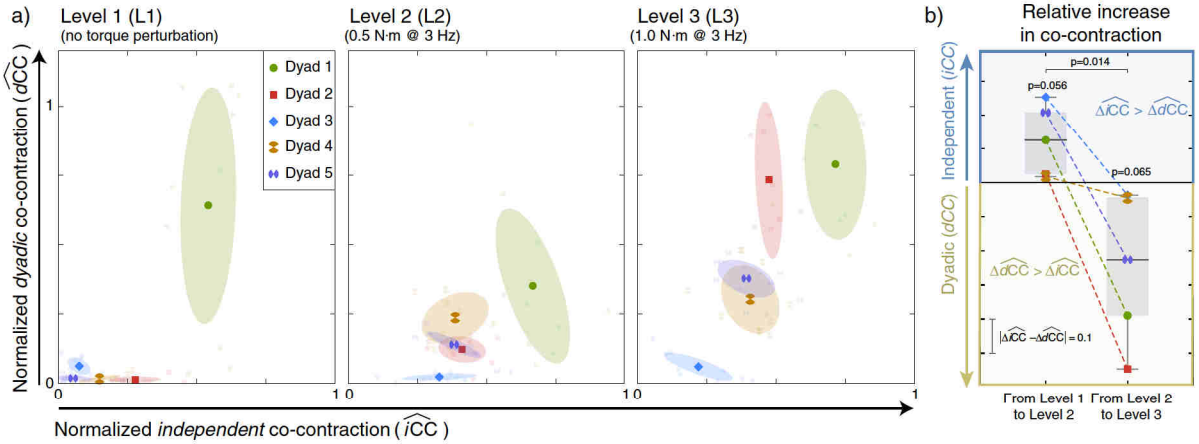

Fig. 7. a) Distribution of normalized *independent* ($\widehat{iCC}$) and *dyadic* ($\widehat{dCC}$) co-contraction. Small markers correspond to the different trials during dyad sessions. Big markers and ellipses correspond to the mean and 95% simultaneous confidence interval respectively. b) When torque perturbations were introduced (Level 2), dyads first preferred to increase $\widehat{iCC}$ levels as opposed to $\widehat{dCC}$; when the magnitude of the perturbation increased further, dyads increased $\widehat{dCC}$ more than $\widehat{iCC}$. The vertical axis shows: $\Delta\widehat{iCC}-\Delta\widehat{dCC}=\left(\widehat{iCC}_{Ln+1}-\widehat{iCC}_{Ln}\right)^{+}-\left(\widehat{dCC}_{Ln+1}-\widehat{dCC}_{Ln}\right)^{+}$. Reported *p*-values are only intended as an indication of the strength of the evidence for each of the comparisons (two sided t-test for $\Delta\widehat{iCC}-\Delta\widehat{dCC}$ comparisons; paired, two sided t-test for the other comparison).

classifier, we could characterize motor interaction strategies that dyads use in undertaking a collaborative tracking task while attenuating mechanical perturbations. We observed that dyads had a general trend to converge to a baseline strategy when no external perturbation was present. This baseline strategy was different for each dyad, suggesting that the solution for the task was not global but specific to each particular dyad. Once external mechanical perturbations were applied, dyads shifted their baseline strategy towards a similar strategy in which pushing or pulling against each other was required.

In addition to interaction torques, we used EMG to gather information about the muscular activity of the partners. Because of muscle redundancy, partners in a dyad can adopt numerous strategies while attempting to mitigate the effects of external noise: e.g. one or both partners can co-contract independently to varying degrees (independent co-contraction, *i*CC) or partners can co-contract by increasing the interaction torque via pulling or pushing against each together (dyadic co-contraction, *d*CC). These strategies involve different energy expenditures and can lead to different results in attenuating outside disturbances, but would produce similar interaction torque patterns. As such, information about muscle activations was necessary to increase our understanding of the roles that each dyad executed. When mechanical perturbation was introduced, dyads showed a tendency to counteract the external disturbances by increasing both *i*CC and *d*CC, but *i*CC with a greater extent. When the perturbation became larger, dyads tended to increase the amount of interaction torque (*d*CC) to a greater extent, even though dyads could have kept co-contracting independently. It is possible that when dyads were presented with a higher perturbation, *d*CC was preferred as opposed to *i*CC in order to reduce the signal dependent noise (e.g. [19,20]), a possibility that may be worth to investigate further.

Other experiments involving dyadic interactions have also reported that dyad partners exert greater interaction forces than those necessary to achieve task goals. In an experiment based on the Prisoner's Dilemma, Braun et al. [21] investigated the tendency of dyads to behave according to game theoretic solutions when their joint effort influenced the dynamics of a force field. Their results suggested that while individuals undertaking the task bimanually settled on solutions which minimized the force requirement, dyad participants adopted approaches that required more force than the complete cooperation case, but also ensured that their amount of force did not depend on the decisions of the other partner in the dyad. Although it is unsurprising that a tug-a-war emerged between partners in a competitive scenario, subjects knowingly collaborating also apply greater interaction forces than necessary to achieve the task. Reed and Peshkin [18] observed dyadic contraction, or a non-negligible difference force, once dyads had reached the target and remained in that position. Indeed, interaction forces between 1.5 and 7.5 N were present in every participating dyad at a stage of the experiment that could be achieved without *any* interaction force. They conjectured that this was for stability reasons, analogous to an individual co-contracting to maintain a position. More recently, van der Wel et al. [22] conducted a study in which dyads or individuals used strings to control the motion of a pendulum and guide it back and forth between two targets: pulling on one string moved the pendulum left and the other, right. Because partners could not apply compressive forces to the pendulum, the scope of strategies was limited to the relative times at which partners apply tensile forces to the string in their respective directions, as well as the relative magnitudes of the forces which are applied. Although individuals and dyads achieved comparable endpoint error, their approaches differed in that dyads displayed much greater force amplification and overlap than did individuals, particularly in tasks with higher coordination requirements. The authors reasoned that the increased force served as a means of strengthening communication between the partners.

Based on our results and in contrast to van der Wel and colleagues' view, we interpret the increase of interaction forces in dyadic interactions as a by-product of unsynchronized forces, underestimation of their partner's forces, or a means of preventing asynchronous motions (or a combination of the three). This behavior is consistent with the work of Shergill et al. [23] who showed that self-generated forces are perceived as weaker than externally-generated forces; this predictive sensory attenuation can affect how one person reacts to the forces produced by the partner, thus leading to force escalation during repetitive physical contact. Furthermore, because the perturbations introduce instability, the cursor position becomes less predictable at any time. Dyad partners lose spatial precision and are less certain about their location relative to the target. If partners are already pushing or pulling, the likelihood of them changing the overall direction of motion is decreased as this would result in an even more asynchronous motion of the target, thus they keep pulling or pushing. Indeed, in a similar bimanual experiment, Reinkensmeyer et al. [24] explored human control of a simple two-hand grasp system, in which subjects were asked to stabilize a pencil-like transducer between their hands while conducting flexion/extension movements in a one-degree-of-freedomdual-wrist manipulandum. Although the task could be achieved without specializations, Reinkensmeyer et al. found that in rightward movements, the right hand contributed most of the accelerating force while the left

hand acted as a brake; the converse was true for movements in the opposite direction. They also found that individuals exerted more force than necessary to stabilize the object, possibly because haptic feedback is comparatively noisy and dropping the object would have meant failing the task.

We still know little about the robustness and formation of such specializations, i.e. whether roles are formed intentionally or its formation is interactive and emergent. Our data using mechanical perturbations suggest the latter; however, to investigate the role formation process and to test the robustness of observed interactive strategies in an environment without mechanical perturbations, we are currently investigating how altered visual feedback can encourage dyads to modify their interaction patterns, using an on-line version of the classifier presented in this paper. Once dyads adopt a particular strategy, we evaluate the stability and robustness of their different approaches.

In terms of dyadic performance, we found that the dyadic performance was, most of the time, better than the performance of the worse partner but worse that the performance of the better partner. Only in few cases, dyadic performance was better than the performance of the better partner. Detailed analysis of performance is out of the scope of this paper and modeling and analysis of these results will be presented elsewhere. However, it is interesting to note that in the experiments presented by Reed et al. [3], physically coupled dyads were frequently better, i.e. faster, than individuals in a target acquisition task. However in another experiment, Reed and Peshkin [18] reported dyads having worse performance than individuals alone in a force attenuation task. On the other hand, the results by Ganesh et al. [8] reported joint interaction that was beneficial for both the worse and the better partner. However, in Ganesh et al. study the connection between the subjects was compliant so that a better individual did not have follow a worse partner, yet may benefit even from this interaction. These differences in conclusions between different studies are likely to be attributed to the differences in the task and therefore, require further investigations.

Acknowledgments

The authors thank Carlo Bagnato, Ganesh Gowrishankar and Atsushi Takagi for fruitful discussions, and Wayne Dailey and Camila Shirota for editing the text. This work was supported by EU grants FP7-ICT-231724 HUMOUR, FP7-ICT-601003 BALANCE and H2020-ICT-23-2014 COGIMON.

Appendix A. Classification of specific strategies based on interaction torques

A simple way to estimate the most probable strategy taken by a dyad during a particular *sweep* (i.e. a full period of the moving target), based solely on interaction torque patterns, is to define a set of functions ("pattern templates") to which the observed interaction torque profiles are compared. As mentioned previously, one could add specificity to these strategies based on the co-contraction levels provided by each partner.

For our particular task, we defined the pattern templates (s_1, …, s_5) as follows:

$$\begin{aligned}
&\text{Drive and brake (D–B)}: && s_1(k) = \sin\left(2\pi f_t \frac{k}{f_s} + \varphi\right)\\
&\text{Drive and stay centered (D–sC)}: && s_2(k) = -\cos\left(2\pi f_t \frac{k}{f_s} + \varphi\right)\\
&\text{Flex and extend (F–E)}: && s_3(k) = \left(\cos\left(4\pi f_t \frac{k}{f_s} + \pi + \varphi\right) + 1\right)/2\\
&\text{Drive and stay flexed (D–sF)}: && s_4(k) = \left(\cos\left(2\pi f_t \frac{k}{f_s} + \pi + \varphi\right) - 1\right)/2\\
&\text{Drive and stay extended (D–sE)}: && s_5(k) = \left(1 - \cos\left(2\pi f_t \frac{k}{f_s} + \pi + \varphi\right)\right)/2
\end{aligned} \tag{10}$$

where f_t corresponds to the moving target frequency [Hz] (for this study $f_t = 0.2$) f_s is the sampling frequency [Hz] (for this study $f_s = 100$), φ is a phase shift [rad] that can be adjusted to the specific periodic task (for this study, $\varphi = 0$, given the descriptions provided in Section 3.1.1), and $k = 1,\ldots,2N$ with N corresponding to the number of data points in a given motion (i.e. 2N for a complete sweep). These functions were proposed as they qualitatively resemble the shape of the observed torque patterns. Note that these templates are ad hoc to our experimental task; however, one could apply the same approach for analyzing other tasks. A pattern template matrix was then defined as:

$$S_{i,k} = \begin{pmatrix} s_1(1) & \cdots & s_1(2N) \\ \vdots & \ddots & \vdots \\ s_5(1) & \cdots & s_5(2N) \end{pmatrix}. \tag{11}$$

To compare the interaction torque pattern of a particular attempt against these templates, the data was pre-processed and normalized. This normalization process was done in order to compensate for the asymmetries that may be present in a given interaction torque pattern (e.g. due to differences in strength between partners or varied impedance during different movement directions). Furthermore, due to the external perturbations, the torque data would contain frequency components corresponding to those of the perturbation.

To remove noise from the signal, in particular the 3 Hz mechanical perturbation, the torque data for each sweep and for each partner, $T^p | p \in \{\text{green, yellow}\}$, was low-pass filtered using a zero-lag second order Butterworth filter (2 Hz cut-off) — step 1, Fig. 5. The signal for the sweep in question was then normalized according to various cases. Sweeps in which all the elements in filtered torque signal had the same sign were normalized as in Eq. (12), whereas sweeps in which both positive and negative torque measurements were present were normalized according to Eq. (13)— step 2, Fig. 5.

$$\hat{T}_k^p = \begin{cases} \dfrac{T_k^p - \min\left(T^p\right)}{\max\left(T^p\right) - \min\left(T^p\right)} & \text{sign}\left(T_k^p\right) \geq 0 \\ \dfrac{T_k^p - \max\left(T^p\right)}{\max\left(T^p\right) - \min\left(T^p\right)} & \text{sign}\left(T_k^p\right) < 0 \end{cases} \quad \forall\ k = 1,\ldots,2N \tag{12}$$

$$\hat{T}_k^p = \begin{cases} \dfrac{T_k^p}{\max\left(T^p\right)} & \text{sign}\left(T_k^p\right) \geq 0 \\ \dfrac{T_k^p}{\left|\min\left(T^p\right)\right|} & \text{sign}\left(T_k^p\right) < 0 \end{cases} \quad \forall\ k = 1,\ldots,2N \tag{13}$$

To smooth out the signal and remove the first derivative discontinuities introduced by the normalization process, the torque data $\hat{T}^p$ was low-pass filtered again using a zero-lag second order Butterworth filter (0.5 Hz cut-off) — step 3, Fig. 5.

The Euclidean distance (A^p) between the normalized torque data vector and each strategy template was then calculated for each partner. The Euclidean distance was also calculated for the reciprocal strategies (A'^p), which corresponds to the case where the other partner in the dyad performs the "driving" action, e.g. s_1 corresponds to green driving and yellow braking, while $-s_1$ corresponds to yellow driving and green braking. These distances can be expressed as:

$$\begin{aligned} A_i^p &= \|S_i - \hat{T}^p\| \\ A'^p_i &= \|-S_i - \hat{T}^p\| \end{aligned} \quad \forall\ i = 1,\ldots,q \tag{14}$$

where q is the number of pattern templates (i.e. $q = 5$ for our case) — step 4, Fig. 5.

Although it may be possible to identify a strategy by using the torque pattern from just one of the partners due to the symmetry on the

interaction torque signals, we decided to calculate these values for both partners and merge them together in a later stage as this would make our estimation more reliable. In this regard, the vectors of Euclidean distances (B^p) for each partner are organized as follows:

$$B^{\text{green}} = \left\{A_1^{\text{green}}, \ldots, A_q^{\text{green}}, A'^{\text{green}}_1, \ldots, A'^{\text{green}}_q\right\}$$
$$B^{\text{yellow}} = \left\{A'^{\text{yellow}}_1, \ldots, A'^{\text{yellow}}_q, A_1^{\text{yellow}}, \ldots, A_q^{\text{yellow}}\right\}. \quad (15)$$

One could then assume that the likelihood that a given partner had adopted a particular strategy during a sweep is inversely proportional to the distance between the template of the strategy in question and that partner's normalized torque vector. In other words, the greater the resemblance between a partner's normalized torque vector and the template of a particular strategy, the more likely (i.e. probable) it is that the partner had adopted that strategy for the sweep in question. Given this assumption, to express a value corresponding to the likelihood of a particular specific strategy for a particular subject (D^p), the Euclidean distance vectors were normalized as follows:

$$C_i^p = \frac{1}{B_i^p}$$
$$D_i^p = \frac{C_i^p}{\sum C^p} \quad \forall\ i = 1, \ldots, 2q. \quad (16)$$

To combine the probabilities from both partners — step 5, Fig. 5, we could use any triangular norm (t-norm), e.g. Einstein product, algebraic product, and minimum, Lukasiewicz t-norm. For simplicity, the algebraic product was used and strategy likelihoods based on interaction torques (E) for both partners were combined in the following form:

$$E = \frac{\text{diag}\left(D^{\text{green}} \otimes D^{\text{yellow}}\right)}{D^{\text{green}}\left(D^{\text{yellow}}\right)^T}. \quad (17)$$

Individual elements of E correspond to the likelihood of a specific strategy based on interaction torques (denoted as p in Fig. 5 and Fig. 6b). The most probable strategy based on interaction torque patterns corresponds to the index in which the maximum value in the vector E occurs.

As mentioned in Section 3.1.1, interpretation solely on interaction torques could be misleading if both partners try to move simultaneously in the direction of the moving target. To include this possibility, we quantified the likelihood of the BT special case in terms of the percentage of the attempt on which the dyad reciprocal activations overlapped. This overlap was quantified in terms of both the sign of each partner's RA and the sign of the first time derivative of each partner's RA as follows:

$$F = \frac{\text{count}\left(\left|\sum_p \text{sign}\left(\text{RA}^p\right)\right| + \left|\sum_p \text{sign}\left(\frac{d\text{RA}^p}{dt}\right)\right|, 4\right)}{2N} \quad (18)$$

where count(•,4) counts the number of occurrences of the number 4 in the vector •. This metric can then be combined with the previous probabilities of partners trying to perform any of the broad strategies as follows:

$$G = \left\{E_1, \ldots, E_{2q}, F\right\}$$
$$H_i = \frac{G_i}{\sum G} \quad \forall\ i = 1, \ldots, 2q+1. \quad (19)$$

The most probable strategy, including the BT special case, is then given by the maximum value in H.

References

[1] M.M. Rahman, R. Ikeura, K. Mizutani, Control characteristics of two humans in cooperative task, SMC 2000 Conference Proceedings: 2000 IEEE International Conference on Systems, Man & Cybernetics 2000, pp. 1301–1306.
[2] S. Gentry, E. Feron, R. Murray-Smith, Human–human haptic collaboration in cyclical Fitts' tasks, 2005 IEEE/RSJ International Conference on Intelligent Robots and Systems (IROS 2005) 2005, pp. 3402–3407.
[3] K. Reed, M. Peshkin, M.J. Hartmann, M. Grabowecky, J. Patton, P.M. Yishton, Haptically linked dyads are two motor-control systems better than one? Psychol. Sci. 17 (2006) 365–366.
[4] N. Stefanov, A. Peer, M. Buss, Role determination in human–human interaction, EuroHaptics conference, 2009 and Symposium on Haptic Interfaces for Virtual Environment and Teleoperator Systems. World Haptics 2009. Third Joint 2009, pp. 51–56.
[5] R. Groten, D. Feth, H. Goshy, A. Peer, D.A. Kenny, M. Buss, Experimental Analysis of Dominance in Haptic CollaborationToyama 2009. 723–729.
[6] A. Melendez-Calderon, V. Komisar, G. Ganesh, E. Burdet, Classification of strategies for disturbance attenuation in human–human collaborative tasks. Engineering in Medicine and Biology Society (EMBC), 2011 Annual International Conference of the IEEE, Boston, MA, USA, 2011.
[7] D. De Santis, J. Zenzeri, L. Masia, V. Squeri, P. Morasso, Human–human physical interaction in the joint control of an underactuated virtual object, Conf Proc IEEE Eng Med Biol Soc 2014, pp. 4407–4410.
[8] G. Ganesh, A. Takagi, R. Osu, T. Yoshioka, M. Kawato, E. Burdet, Two is better than one: physical interactions improve motor performance in humans, Sci. Rep. 4 (2014) 01/23/online.
[9] A. Sawers, L.H. Ting, Perspectives on human–human sensorimotor interactions for the design of rehabilitation robots, J Neuroeng Rehabil 11 (2014) 142.
[10] E. Burdet, R. Osu, D.W. Franklin, T.E. Milner, M. Kawato, The central nervous system stabilizes unstable dynamics by learning optimal impedance, Nature 414 (2001) 446–449.
[11] L.P. Selen, J.H. van Dieen, P.J. Beek, Impedance modulation and feedback corrections in tracking targets of variable size and frequency, J. Neurophysiol. 96 (Nov 2006) 2750–2759.
[12] D.W. Franklin, G. Liaw, T.E. Milner, R. Osu, E. Burdet, M. Kawato, Endpoint stiffness of the arm is directionally tuned to instability in the environment, J Neurosci 27 (Jul 18 2007) 7705–7716.
[13] L. Summers, J. Shannon, T. White, R. Shiner, Fly-by-wire sidestick controller evaluation, SAE Technical Paper, 1987.
[14] A. Melendez-Calderon, L. Bagutti, B. Pedrono, E. Burdet, Hi5: a versatile dual-wrist device to study human–human interaction and bimanual control, IEEE/RSJ international conference on Intelligent robots and systems, San Francisco, USA, 2011.
[15] T. Flash, N. Hogan, The coordination of arm movements: an experimentally confirmed mathematical model, J Neurosci 5 (Jul 1985) 1688–1703.
[16] D.J. Saville, Multiple comparison procedures: the practical solution, Am. Stat. 44 (1990) 174–180.
[17] K.B. Reed, M. Peshkin, M.J. Hartmann, J. Edward Colgate, J. Patton, Kinesthetic InteractionChicago, IL 2005. 569–574.
[18] K.B. Reed, M.A. Peshkin, Physical collaboration of human–human and human–robot teams, IEEE Transactions on Haptics 1 (2008) 108–120.
[19] L.P. Selen, D.W. Franklin, D.M. Wolpert, Impedance control reduces instability that arises from motor noise, J Neurosci 29 (Oct 7 2009) 12606–12616.
[20] A.A. Faisal, L.P. Selen, D.M. Wolpert, Noise in the nervous system, Nat. Rev. Neurosci. 9 (Apr 2008) 292–303.
[21] D.A. Braun, P.A. Ortega, D.M. Wolpert, Nash equilibria in multi-agent motor interactions, PLoS Comput. Biol. 5 (2009) e1000468.
[22] R.P. van der Wel, G. Knoblich, N. Sebanz, Let the force be with us: dyads exploit haptic coupling for coordination, J Exp Psychol Hum Percept Perform (Mar 21 2011).
[23] S.S. Shergill, P.M. Bays, C.D. Frith, D.M. Wolpert, Two eyes for an eye: the neuroscience of force escalation, Science 301 (2003) 187 July 11, 2003.
[24] D.J. Reinkensmeyer, P.S. Lum, S.L. Lehman, Human control of a simple two-hand grasp, Biol. Cybern. 67 (1992) 553–564.